Soil Dynamics and Earthquake Engineering 87 (2016) 116–124

Contents lists available at ScienceDirect

Soil Dynamics and Earthquake Engineering

journal homepage: www.elsevier.com/locate/soildyn

Wavelet-based generation of spatially correlated accelerograms

Kaushik Sarkar, Vinay K. Gupta *, Riya C. George

Department of Civil Engineering, Indian Institute of Technology Kanpur, Kanpur 208016, India

ARTICLE INFO

Article history:
Received 24 August 2015
Received in revised form
16 March 2016
Accepted 9 May 2016
Available online 1 June 2016

Keywords:
Spatial correlation
Accelerogram simulation
Wavelet analysis
Stochastic decomposition
Design spectrum
Coherency structure

ABSTRACT

For the seismic analysis of complex or nonlinear extended structures, it is useful to generate a set of properly correlated earthquake accelerograms that are consistent with a specified seismic hazard. A new simulation approach is presented in this paper for the generation of ensembles of spatially correlated accelerograms such that the simulated motions are consistent with (i) a parent accelerogram in the sense of temporal variations in frequency content, (ii) a design spectrum in the mean sense, and (iii) with a given instantaneous coherency structure. The formulation is based on the extension of stochastic decomposition technique to wavelet domain via the method of spectral factorization. A complex variant of the modified Littlewood-Paley wavelet function is proposed for the wavelet-based representation of earthquake accelerograms, such that this explicitly brings out the phase information of the signal, besides being able to decompose it into component time-histories having energy in non-overlapping frequency bands. The proposed approach is illustrated by generating ensembles of accelerograms at four stations.

1. Introduction

The primary concern in the analysis and design of structures for the effects of strong earthquakes is the proper definition and representation of the design ground motion. Among different approaches used to this end, those via response spectrum or power spectral density function (PSDF) are most common. However, in several applications, such as performance evaluation of mathematical models of structures for design level motions, experimental verification of new design concepts, and statistical analyses of complex and nonlinear structures, it is required to have a time-description of the desired ground motion. In most cases, the available recorded ground motions may not meet the necessary design specifications for a given site. Therefore, there remains a need for the simulation of artificial ground motions compatible with the design requirements.

For the analyses of spatially extended structures, such as long-span bridges, pipelines or even a simple building system with raft foundation, it is required to account for possible variations in the earthquake ground motion at different points in space. Spatial variability in seismic ground motions can result from a number of causes, such as, wave passage effect, incoherence effect, extended source effect, attenuation effect etc. The spatial variability of ground motions has been estimated and modeled stochastically by using the strong motions recorded at dense instrument arrays. Ground motions at different stations are typically considered to be the realizations of space-time random fields. Spatial variability is characterized by the coherency function, which is defined for any two homogeneous random processes in terms of their smoothed cross-PSDF and individual PSDFs. Based on the regression analyses of the data available from the dense instrument arrays (SMART-1 array, LSST array, etc.), a number of empirical and semi-empirical models have been proposed for the coherency function [1–13].

Generation of spatially correlated accelerograms has been attempted by several researchers. The techniques used for this purpose include spectral factorization [7,14–17], covariance matrix decomposition [18], auto-regressive moving average (ARMA) approximation [19], sinusoid superposition [20,21], fast Fourier transform and digital filtering-based methods [22,23], and conditional simulation [24–27]. The main objective in these simulation schemes was that the statistical properties of the simulated motions matched with those of the target random field. Some of these schemes have used the method of stochastic decomposition suggested by Shinozuka [28]. Hao et al. [7] generated a set of correlated time histories by using the summation of trigonometric series. Li and Kareem [22] used time-dependent weighing functions in the stochastic decomposition, while the target ground motion characteristics were specified in terms of an evolutionary spectral matrix. Shrikhande and Gupta [17] generated spatially correlated time histories by using the nonstationary characteristics of a given accelerogram. Zerva [29] has reviewed various schemes

* Corresponding author.
E-mail address: vinaykg@iitk.ac.in (V.K. Gupta).

http://dx.doi.org/10.1016/j.soildyn.2016.05.005
0267-7261/

of simulation of ground motions in detail.

In most of the above simulation procedures, except for those proposed by Li and Kareem [22] and Shrikhande and Gupta [17], generated time histories were modulated with the help of a deterministic envelope function. However, the envelope function and phase spectrum of a time-history are known to be closely related [30,31], and therefore, such modulation may change the phase properties arbitrarily, thus disturbing the coherency structure. Also, it is unrealistic to model a complex phenomenon like earthquake ground motion via a deterministic modulating function. The scheme proposed by Shrikhande and Gupta [17] incorporates nonstationarity in the simulation procedure itself by using the phase and duration spectra of a recorded time-history, thus requiring no post-processing of the simulated motions and keeping the coherency structure intact. However, this scheme does not account for temporal variations in the coherency structure. Also, the energy distributions in the target spectrum and the parent accelerogram need to be "not too different".

There have been several attempts in the recent years that have focused on simulating more realistic spatially correlated accelerograms. Bi and Hao [32] approximately simulated the spatially varying ground motions at an uneven site with nonuniform soil conditions. Konakli and Der Kiureghian [33] simulated nonstationary ground motions considering the effects of incoherence, wave passage and differential site response. Cacciola and Deodatis [34] illustrated the simulation of ground motions at stations with different soil conditions and separated by 30–50 m of distance. Zhang et al. [35] simulated tri-directional nonstationary accelerograms at varying site conditions by considering power spectra at the bed rock and the site amplification of P-, SV- and SH-waves. In a more recent publication, Shields [36] simulated spectrum-compatible, uniformly modulated nonstationary accelerograms by upgrading the evolutionary power spectral density function with random pulse-like perturbations.

Considering that nonstationarity is directly linked to temporal variations in the characteristics of a signal, a time-frequency transformation tool is needed to simulate realistic accelerograms. For example, Wen and Gu [37] simulated nonstationary processes based on Hilbert spectra. The development of wavelet transform technique has however made it possible to represent the temporal variations in the frequency content of a signal more elegantly. The wavelet transform technique is more versatile than the other time-frequency localizing techniques, like Gabor transform, short-time Fourier transform, etc., due to its flexible time-frequency windowing feature [38]. Besides several important engineering applications [39–45], this technique has already been used by [46,47] for the characterization of design ground motions. Zeldin and Spanos [48] synthesized random fields using wavelets. Spanos and Failla [49] and Huang and Chen [50] estimated the evolutionary spectra using wavelet transforms. Iyama and Kuwamura [51] and Gurley and Kareem [52] simulated ground motions using wavelet transforms. Cecini and Palmeri [53] and Giaralis and Spanos [54] simulated spectrum-compatible accelerograms using harmonic wavelets. Huang [55] simulated nonlinear spatially variable ground motions using wavelets and spectral representation method.

In this study based on the thesis of the first author [56], a wavelet-based procedure is formulated for simulating the ensembles of spatially correlated accelerograms, such that those are compatible with a given response spectrum and an assumed coherency model. An analytic function is considered as the mother wavelet function and the popular stochastic decomposition technique is extended to the wavelet domain for this purpose. The proposed approach is illustrated by generating a set of ensembles of correlated accelerograms for the stations 100, 200 and 300 m apart.

2. Wavelet transform

2.1. Brief review

If $f(t)$ is a function belonging to $L^2(R)$ space, the continuous wavelet transformation of $f(t)$ with respect to a mother wavelet function $\psi(t)$ is defined as [38,57]

$$W_\psi f(a, b) = \int_{-\infty}^{\infty} f(t)\psi_{a,b}^*(t)\mathrm{d}t \tag{1}$$

with

$$\psi_{a,b}(t) = \frac{1}{\sqrt{|a|}}\psi\left(\frac{t-b}{a}\right) \tag{2}$$

where a and b are real-valued scale and shift parameters, respectively, and the asterisk denotes complex conjugation. The transient nature and finite energy content of the earthquake signals make it possible to have their wavelet domain representation. It is possible to reconstruct the original signal $f(t)$ from its wavelet coefficients $W_\psi f(a, b)$ as

$$f(t) = \frac{1}{2\pi C_\psi}\int_{-\infty}^{\infty}\int_{-\infty}^{\infty}\frac{1}{a^2}W_\psi f(a, b)\psi_{a,b}(t)\mathrm{d}a\mathrm{d}b \tag{3}$$

with

$$C_\psi = \int_{-\infty}^{\infty}\frac{\left|\hat{\psi}(\omega)\right|^2}{|\omega|}\mathrm{d}\omega \tag{4}$$

and

$$\hat{\psi}(\omega) = \frac{1}{\sqrt{2\pi}}\int_{-\infty}^{\infty}\psi(t)e^{-i\omega t}\mathrm{d}t \tag{5}$$

denoting the Fourier transform of $\psi(t)$.

2.2. Mother wavelet

The choice of mother wavelet depends on the type of application and the type of function being analyzed. The most common transformation technique, that is Fourier transformation, uses a complex basis function, $e^{i\omega t}$. This function consists of a real (cosine) function added in quadrature to its Hilbert transform (i.e., sine function). Due to this, $e^{i\omega t}$ belongs to a special class of complex functions, called analytic functions, which have non-zero spectra only for positive frequencies [58]. The use of an analytic function as the basis function entails it to reveal the phase information of a signal, and therefore, Fourier transform is considered to be useful for deriving the phase properties of stationary signals. Unlike the Fourier transformation, a wavelet transformation uses a time-localized oscillatory function as the analyzing or mother wavelet, which can be either real or complex. Both real and complex mother wavelets perform a complete and reversible transformation of a signal from time domain to wavelet domain with no information loss, but in the case of real wavelets, the phase-related information of the signal cannot be separated out from the transformed signal. It is therefore necessary that whenever instantaneous phase properties of a signal are explicitly required, a complex mother wavelet, which is also an analytic function, is used [58].

Another important characteristic of the mother wavelet function is its resolution. In this respect, the mother wavelet proposed by Basu and Gupta [41] is well suited to deal with earthquake signals. This function is basically a modified version of the Littlewood-Paley (L-P) wavelet function, with improved resolution in frequency domain. The advantage of the L-P basis function is that its Fourier spectrum is constant over a specific band of frequencies and zero for all other frequencies. However, with the original

parameters of the L-P basis function, this band was found to be too large for accurately representing the energy distribution of recorded earthquake ground motions. The modified function has the same band-limited feature, but here the width of each band is reduced significantly. Though this function is adequate for an input-output stochastic formulation for structural systems, this, being a real function, cannot reveal the phase characteristics of a signal. Therefore, a variant of the modified function is considered in this study.

The mother wavelet proposed by Basu and Gupta [41] is defined as

$$\psi(t) = \frac{\sin(\sigma\pi t) - \sin(\pi t)}{\pi t\sqrt{\sigma - 1}} \tag{6}$$

with σ taken as $2^{1/4}$ in the case of earthquake accelerograms. On shifting the phase of this function by $\pi/2$, the Hilbert transform of the function is obtained as

$$\bar{\psi}(t) = \frac{\cos(\pi t) - \cos(\sigma\pi t)}{\pi t\sqrt{\sigma - 1}} \tag{7}$$

On adding Eq. (7) to Eq. (6) in quadrature, the analytic equivalent of modified L-P wavelet is obtained as

$$\psi(t) = \frac{e^{i\sigma\pi t} - e^{i\pi t}}{i\pi t\sqrt{\sigma - 1}} \tag{8}$$

This (complex) function is proposed to be used as the mother wavelet in this study (with $\sigma = 2^{1/4}$).

Fig. 1 shows the real and imaginary parts of the mother wavelet used. The Fourier transform of this function is

$$\hat{\psi}(\omega) = \frac{2}{\sqrt{2(\sigma - 1)\pi}}; \quad \pi < \omega < \sigma\pi$$
$$= 0; \quad \text{otherwise} \tag{9}$$

which is twice as much as the Fourier transform of the modified L-P wavelet. The mother wavelet considered here may also be seen as a modification of the harmonic wavelet basis [39], just as the L-P basis was modified by Basu and Gupta [41]. The real part of this mother wavelet is the modified L-P wavelet itself, and therefore this inherits the advantages of the modified L-P wavelet and is as much relevant to the seismic applications as is the modified L-P wavelet. Hence, different scale parameters would correspond to different non-overlapping frequency bands with the use of the mother wavelet considered, and a given signal can be expressed as a linear combination of several signals having energy in non-overlapping frequency bands. Further, the widths of these bands being sufficiently small (due to the use of $\sigma = 2^{1/4}$), the mid-frequency of a band can be treated as the representative frequency for that band. The temporal information in each of the band-limited signals can be obtained by changing the shift parameter.

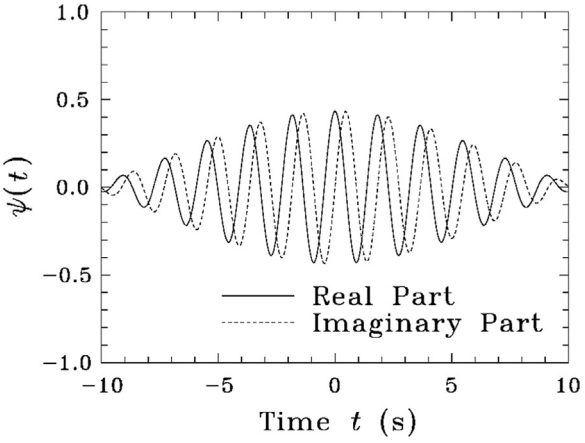

Fig. 1. Real and imaginary parts of the mother wavelet used.

To evaluate the integrals in Eqs. (6) and (7), a discretization scheme used by Basu and Gupta [41] is adopted here. Most of the modern accelerograms are recorded as discrete time ordinates separated by a constant time interval, and hence, it is useful to have discretized versions of the integrals. According to the discretization scheme of Basu and Gupta [41], $a_j = \sigma^j$ and $b_i = (i-1)\Delta b$, where Δb is the sampling time-interval of the accelerogram (taken as 0.02 s in this study). Hence,

$$\Delta b_i = \left[(b_{i+1} - b_i) + (b_i - b_{i-1})\right]/2 = \Delta b \tag{10a}$$

and

$$\Delta a_j = \left[\left(a_{j+1} - a_j\right) + \left(a_j - a_{j-1}\right)\right]/2 = \frac{a_j}{2}\left(\sigma - \frac{1}{\sigma}\right) \tag{10b}$$

Also, a and b are now parameterized with the help of two other variables, i and j. Using the above two relations, the discretized versions of Eqs. (1) and (3) may be obtained as [41]

$$W_\psi f(a_j, b_i) = \frac{1}{\sqrt{a_j}}\int_{-\infty}^{\infty} f(t)\psi^*\left(\frac{t - b_i}{a_j}\right)dt \tag{11}$$

and

$$f(t) = \frac{K\Delta b}{a_j}\mathrm{Re}\left[\sum_i\sum_j W_\psi f(a_j, b_i)\psi\left(\frac{t - b_i}{a_j}\right)\right] \tag{12}$$

where Re [.] denotes the real part of [.], and

$$K = \frac{1}{4\pi C_\psi}\left(\sigma - \frac{1}{\sigma}\right) \tag{13}$$

2.3. Synthetic accelerogram with the mother wavelet considered

As mentioned above, the mother wavelet considered is a generalized version of the modified L-P wavelet proposed by Basu and Gupta [41]. Consequently, all the existing formulations with the modified L-P wavelet [41,43,46,47] will hold good for the mother wavelet considered also. In particular, the decomposition of a signal into the constituent 'band-limited' signals and reconstruction of the original signal from those with the help of the mother wavelet considered would give exactly the same results as obtained by the modified L-P wavelet. In view of this, the methodology proposed by Mukherjee and Gupta [46] to generate spectrum-compatible accelerograms in modification of a given accelerogram may be used, as it is, in the case of the mother wavelet considered also. This methodology is briefly summarized in Appendix A and will be used in this paper. For illustration, the accelerogram recorded at Los Angeles fire station, California, USA during the 1994 Northridge Earthquake is made spectrum-compatible by using the mother wavelet considered. The target spectrum considered for this purpose is 5% USNRC design spectrum with the peak ground acceleration of 0.25g. Figs. 2 and 3 show the recorded and modified time-histories respectively. Fig. 4 shows the comparison of the target (pseudo-spectral acceleration) spectrum with the spectrum for the modified accelerogram after 8 iterations.

3. Simulation of spatially correlated accelerograms

In the case of several related processes observed simultaneously, it is convenient to group those together in the form of a

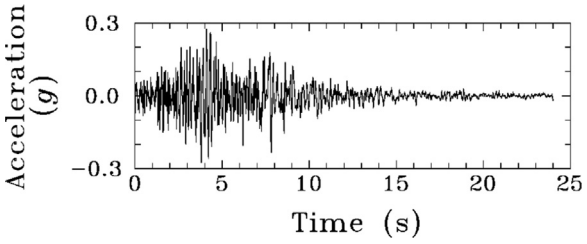

Fig. 2. Real original (recorded) accelerogram.

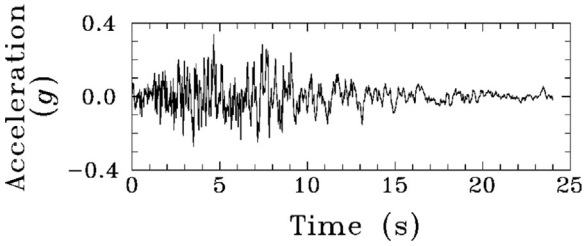

Fig. 3. Modified (spectrum-compatible) accelerogram.

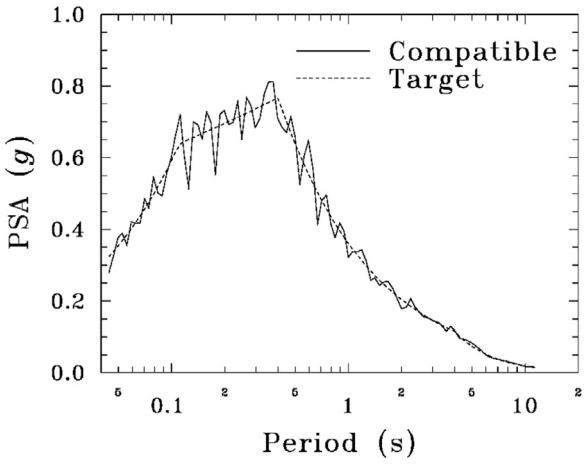

Fig. 4. Comparison of the response spectrum for the modified accelerogram with the target spectrum.

vector. This group is collectively called as vector or multivariate process. The problem of simulation of spatially correlated time-histories is thus a multivariate simulation problem, as each of the ground motion records at different stations is basically a realization of the same event. The most widely used technique for such a simulation is the stochastic decomposition technique, which was originally proposed by Shinozuka [28]. This technique works by decomposing the elements of a parent random process into its constituent sub-processes, either by eigensystem decomposition [59] or by spectral factorization [7,14,17,22]. In this study, the method of spectral factorization is considered to extend the stochastic decomposition technique to the wavelet domain. The main idea of the spectral decomposition technique lies in the factorization of the original spectral matrix of the vector process by Cholesky decomposition into upper and lower triangular matrices. Shinozuka [60] has shown that the spectral matrices of seismic ground motions are usually Hermitian and positive definite within a range of frequencies, and hence the existence of Cholesky factors is ensured. Next, from these Cholesky factors, each of the sub-processes of the elements is simulated sequentially.

Let $\mathbf{F}(t)$ denote the random multivariate process of spatially correlated time-histories at n stations. When $\mathbf{F}(t)$ is stationary, the spectral matrix for this process is defined as

$$\mathbf{S}_{\mathbf{F}}(\omega) = \begin{bmatrix} S_{11}(\omega) & S_{12}(\omega) & \cdot & S_{1n}(\omega) \\ S_{21}(\omega) & S_{22}(\omega) & \cdot & S_{2n}(\omega) \\ \cdot & \cdot & \cdot & \cdot \\ S_{n1}(\omega) & S_{n2}(\omega) & \cdot & S_{nn}(\omega) \end{bmatrix} \tag{14}$$

where, the ith diagonal term denotes the PSDF of the ith element of $\mathbf{F}(t)$ (corresponding to the ground motion process at the ith station) and the (i, j)th off-diagonal term refers to the cross-PSDF between the ith and jth elements of $\mathbf{F}(t)$. The cross-PSDFs between the motions at different pairs of stations reflect the ground-motion variability in a quantitative way. While it is popular to obtain the PSDFs simply by considering the spectrum-compatible PSDFs at the stations under consideration, each of the cross-PSDFs is obtained via the desired correlation between the motions at the corresponding pair of stations. This correlation is characterized by a coherency function which is normalized cross-PSDF with respect to the PSDFs for motions at the corresponding pair of stations (see Appendix B for details).

In order to consider the inherent nonstationarity in the seismic ground motions, the spectral matrix $\mathbf{S}_{\mathbf{F}}(\omega)$ of the target process is proposed to be estimated instantaneously in the form of a series of instantaneous spectral matrices. The target instantaneous matrices will be estimated through a wavelet-based characterization of $\mathbf{F}(t)$, due to the time-localization property of wavelets, and by the use of a suitable coherency function along with the spectrum-compatible instantaneous PSDFs. This aspect will be discussed next, followed by an extension of the stochastic decomposition technique to the wavelet domain, in order to simulate the realizations of different elements of the vector process, $\mathbf{F}(t)$.

3.1. Estimation of Instantaneous Spectral Matrices

It is an accepted practice to characterize the seismic hazard at a site by specifying a single set of smooth design spectra for different damping ratios. Therefore, the ground motions to be simulated at different stations should conform to the same (specified) spectra, particularly when the site is not very large and thus the local (spatial) variations in the design spectra may be neglected. It is proposed to first generate an accelerogram compatible with one of the design spectrum (corresponding to the damping ratio of the structural system) and then to obtain the instantaneous PSDFs from the wavelet coefficients of the generated accelerogram.

It is proposed to generate the spectrum-compatible accelerogram following the procedure of Mukherjee and Gupta [46], even though any of the methods available for synthesizing fully nonstationary, spectrum-compatible ground motions [for example, [34,46,53,61–63]] may be used. For this purpose, it is assumed that a suitable (parent) accelerogram conforming to the local source and site conditions is available. It may be noted that during the modification of the parent accelerogram, the temporal variation of frequency content would remain undisturbed, and hence, the generated (spectrum-compatible) accelerogram would contain the same nonstationary characteristics as in the parent accelerogram.

The instantaneous PSDFs are proposed to be estimated from the generated accelerogram by using the expression given by Basu and Gupta [41] (also see Eq. (22) in the following). In the absence of a number of realizations, ensemble averaging will be carried out through the smoothing of various PSDFs. As discussed above, these instantaneous PSDFs will be applicable for the motions at all stations, and thus, all diagonal terms of the instantaneous spectral matrix will be identical. To estimate the off-diagonal terms of the spectral matrix, say the instantaneous cross-PSDF between the motions at stations m and n, the instantaneous PSDF needs to be multiplied with the corresponding instantaneous coherency function, $\gamma(r_{mn}, \omega, t)$. This function is invariant of time in the case of

stationary processes, and several functional forms exist for the time-invariant function. However, no functional model is available yet for the instantaneous coherency function. Hence, it will be assumed in this study for the purpose of illustration that the coherency function is time-invariant and thus the coherency models available at present may be used to describe the correlations at all time-instants. Though any of the available (time-independent) coherency model could be chosen, the more popular coherency model proposed by Harichandran and Vanmarcke [2] will be used in this study. A brief description of this coherency function is given in Appendix B.

3.2. Proposed formulation

Before we extend the method of stochastic decomposition to simulate accelerograms conforming to the (target) instantaneous spectral matrices of previous sub-section, it is desirable that the expression for (instantaneous) cross-PSDF is formulated in terms of the wavelet coefficients of the realizations of two different elements of $\mathbf{F}(t)$. The expression for the (instantaneous) PSDF of a single element has been already obtained by Basu and Gupta [41] (see Eq. (22)).

For any two time-histories, $X(t)$ and $Y(t)$ that belong to the $L^2(R)$ space, the resolution of identity proposition states that [38]

$$\int_{-\infty}^{\infty} X(t)Y(t)\mathrm{d}t = \frac{1}{2\pi C_\psi}\int_{-\infty}^{\infty}\int_{-\infty}^{\infty}\frac{W_\psi X(a,b)W_\psi^* Y(a,b)}{a^2}\mathrm{d}a\mathrm{d}b \tag{15}$$

For these two time-histories, the Parseval's theorem also gives

$$\int_{-\infty}^{\infty} X(t)Y(t)\mathrm{d}t = \int_{-\infty}^{\infty} X(\omega)Y^*(\omega)\mathrm{d}\omega \tag{16}$$

provided both $X(t)$ and $Y(t)$ belong to the $L^1(R)$ and $L^2(R)$ spaces. This condition is satisfied in the case of earthquake accelerograms. Thus, on comparing Eqs. (15) and (16), one gets

$$\int_{-\infty}^{\infty} X(\omega)Y^*(\omega)\mathrm{d}\omega = \frac{1}{2\pi C_\psi}\int_{-\infty}^{\infty}\int_{-\infty}^{\infty}\frac{W_\psi X(a,b)W_\psi^* Y(a,b)}{a^2}\mathrm{d}a\mathrm{d}b \tag{17}$$

On using the discretization scheme mentioned earlier, Eq. (17) becomes

$$\int_{-\infty}^{\infty} X(\omega)Y^*(\omega)\mathrm{d}\omega = \sum_i\sum_j \frac{K\Delta b}{a_j} W_\psi X(a_j,b_i)W_\psi Y^*(a_j,b_i) \tag{18}$$

Now, on using the property of the wavelet basis function, i.e., $\int_{-\infty}^{\infty}\left|\hat{\psi}_{a_j,b_i}(\omega)\right|^2\mathrm{d}\omega = 1$ and also the non-overlapping band-limited feature of the mother wavelet considered, Eq. (18) may be expressed as

$$\int_{\pi/a_j}^{\sigma\pi/a_j} X(\omega)Y^*(\omega)\mathrm{d}\omega = \int_{\pi/a_j}^{\sigma\pi/a_j}\sum_i \frac{K\Delta b}{a_j} W_\psi X(a_j,b_i)W_\psi Y^*(a_j,b_i)\left|\hat{\psi}_{a_j,b_i}(\omega)\right|^2\mathrm{d}\omega \tag{19}$$

for a particular frequency band corresponding to the scale parameter j. Next, the frequency band $(\pi/a_j, \sigma\pi/a_j)$ being small enough, the integration in this equation is performed in a very small range, and hence the integrands on both sides can be assumed to be equal without much error. Therefore, Eq. (19) gives

$$X(\omega)Y^*(\omega) = \sum_i \frac{K\Delta b}{a_j} W_\psi X(a_j,b_i)W_\psi Y^*(a_j,b_i)\left|\hat{\psi}_{a_j,b_i}(\omega)\right|^2; \quad \frac{\pi}{a_j}\le\omega\le\frac{\sigma\pi}{a_j} \tag{20}$$

On taking expectation of both sides and on using the time localization property of the wavelets, the instantaneous cross-PSDF for the two processes $\mathbf{X}(t)$ and $\mathbf{Y}(t)$ may be expressed as

$$S_{XY}(\omega_j)|_{t=b_i} = \frac{K}{a_j}E[W_\psi X(a_j,b_i)W_\psi Y^*(a_j,b_i)]|\hat{\psi}_{a_j,b_i}(\omega_j)|^2 \tag{21}$$

where ω_j is a frequency (between π/a_j and $\sigma\pi/a_j$) corresponding to the jth scale parameter. For $\mathbf{Y}(t)=\mathbf{X}(t)$, when both processes are same, the expression for the PSDF of either of the two processes comes out to be

$$S_X(\omega_j)|_{t=b_i} = \frac{K}{a_j}E[|W_\psi X(a_j,b_i)|^2]|\hat{\psi}_{a_j,b_i}(\omega_j)|^2 \tag{22}$$

which is the same as obtained earlier by Basu and Gupta [41].

Now, we extend the spectral decomposition method to the wavelet domain and decompose each of the elements of the multivariate process $\mathbf{F}(t)$ into the constituent sub-processes. Without any loss of generality, the mth element of $\mathbf{F}(t)$ can be assumed to be composed of m number of random sub-processes [7,17]. This leads to

$$F_m(t) = \sum_{r=1}^{m} F_{mr}(t) \tag{23}$$

where $F_{mr}(t)$ is a realization of the rth sub-process at the station m. On taking the wavelet transform of both sides, Eq. (23) may be expressed as

$$W_\psi F_m(a_j,b_i) = \sum_{r=1}^{m} A_{mr}(a_j,b_i)e^{i(\phi_{mr}(a_j,b_i)+\phi_{\text{initial}}(a_j,b_i)+\alpha_r)} \tag{24}$$

where $W_\psi F_m(a_j,b_i)$ is the wavelet coefficient of $F_m(t)$, and $A_{mr}(a_j,b_i)$ and $(\phi_{mr}(a_j,b_i)+\phi_{\text{initial}}(a_j,b_i)+\alpha_r)$ are respectively the amplitude and argument of the wavelet coefficient of $F_{mr}(t)$ corresponding to the jth scale and ith instant. Here, α_r is a random phase angle, varying with the sub-process r and being uniformly distributed over the range 0–2π; $\phi_{\text{initial}}(a_j,b_i)$ is the phase angle of the generated spectrum-compatible accelerogram (corresponding to the jth scale and ith instant) and is obtained as the argument of the wavelet coefficients of this motion (see Eq. (11)); and $A_{mr}(a_j,b_i)$ and $\phi_{mr}(a_j,b_i)$ are the deterministic quantities to be obtained from the instantaneous spectral matrix of $\mathbf{F}(t)$, as will be shown below.

Eq. (24) may be used to express $W_\psi F_m(a_j,b_i)W_\psi F_n^*(a_j,b_i)$ in terms of the amplitudes and arguments of the wavelet coefficients of the realizations of $\mathbf{F}_m(t)$ and $\mathbf{F}_n(t)$. On taking the expectation of both sides, one gets

$$E[W_\psi F_m(a_j,b_i)W_\psi F_n^*(a_j,b_i)] = E\left[\sum_{r=1}^{m}\sum_{s=1}^{n} A_{mr}(a_j,b_i)A_{ns}(a_j,b_i)e^{i(\phi_{mr}(a_j,b_i)-\phi_{ns}(a_j,b_i)+\alpha_r-\alpha_s)}\right] \tag{25}$$

Assuming that the constituting sub-processes of a particular element are statistically independent of each other, i.e., the random phase angles α_r and α_s are statistically independent for all $r\neq s$ [14,17], Eq. (25) may be simplified to

$$E[W_\psi F_m(a_j,b_i)W_\psi F_n^*(a_j,b_i)] = \sum_{r=1}^{m} A_{mr}(a_j,b_i)A_{nr}(a_j,b_i)e^{i(\phi_{mr}(a_j,b_i)-\phi_{nr}(a_j,b_i))} \tag{26}$$

for $m \le n$. On considering the instantaneous cross-PSDF for $\mathbf{F}_m(t)$ and $\mathbf{F}_n(t)$, as in Eq. (21), and on substituting Eq. (26), one gets

$$S_{mn}(\omega_j)|_{t=b_i} = \frac{K}{a_j}|\hat{\psi}_{a_j,b_i}(\omega_j)|^2 \sum_{r=1}^{m} A_{mr}(a_j, b_i)A_{nr}(a_j, b_i) e^{i(\phi_{mr}(a_j,b_i)-\phi_{nr}(a_j,b_i))} \quad (27)$$

As discussed earlier, the simulated accelerograms should conform to the target spectral matrix. On Cholesky decomposition, this matrix may be expressed as

$$\mathbf{S}_{\mathbf{F}}(\omega)|_{t=b_i} = L(\omega)|_{t=b_i} \cdot L^H(\omega)|_{t=b_i} \quad (28)$$

where $L(\omega)|_{t=b_i}$ denotes the (complex) lower triangular factor of the spectral matrix at the time instant $t = b_i$, and $L^H(\omega)|_{t=b_i}$ is the transpose of the complex conjugate of $L(\omega)|_{t=b_i}$. Eq. (28) leads to the (m, n)th element of the target spectral matrix in terms of Cholesky factors as [17]

$$S_{mn}(\omega_j)|_{t=b_i} = \sum_{r=1}^{m} L_{mr}(\omega_j)|_{t=b_i} \cdot L^*_{nr}(\omega_j)|_{t=b_i} \quad (29)$$

for $m \le n$, where $L_{mr}(\omega_j)|_{t=b_i}$ denotes the (m, r)th element of $L(\omega)|_{t=b_i}$ (at a frequency ω_j of the jth frequency band), and $L^*_{nr}(\omega_j)|_{t=b_i}$ is the complex conjugate of the (n, r)th element of the same matrix. A term-by-term comparison of the right-hand side expressions of Eqs. (27) and (29) gives

$$A_{mr}(a_j, b_i) = \sqrt{\frac{a_j}{K}} \frac{1}{|\hat{\psi}_{a_j,b_i}(\omega_j)|} |L_{mr}(\omega_j)|_{t=b_i}| \quad (30a)$$

and

$$\phi_{mr}(a_j, b_i) = \tan^{-1} \frac{\mathrm{Im}(L_{mr}(\omega_j)|_{t=b_i})}{\mathrm{Re}(L_{mr}(\omega_j)|_{t=b_i})} \quad (30b)$$

where Im(.) and Re(.) respectively denote the imaginary and real parts of the complex element inside the parenthesis.

It may be observed that the simulation of the elements of the (multivariate) ground motion process primarily involves the estimation of the wavelet coefficients of the constituting sub-processes of each of the elements from the Cholesky factors of the (instantaneous) target spectral matrix. Once these quantities are obtained from Eqs. (30a) and (30b), those are used in Eq. (24) along with the statistically independent random phase angles to generate the wavelet coefficients of the realizations of the individual elements of $\mathbf{F}(t)$. These coefficients are then inverse-transformed (see Eq. (12)) to obtain the corresponding time-histories. The use of different sets of random phase angles leads to the generation of ensembles.

4. Illustration of the proposed procedure

The proposed approach is illustrated by synthesizing accelerograms at four stations, 100 m apart, such that those have the nonstationary characteristics of the recorded motion during the 1994 Northridge earthquake as in Fig. 2. The example motion is first made spectrum-compatible, so as to be consistent with the 5% USNRC design spectrum of 0.25g peak ground acceleration [46], and then the instantaneous PSDFs are estimated from these motions. For this, wavelet coefficients of the motion are computed with the help of Eq. (11), and then Eq. (22) is used along with the smoothing operation (to take care of the expectation operator). Fig. 5 shows the instantaneous PSDFs at three arbitrarily chosen instants for the example motion. The parameters of the coherency function (see Appendix B) are considered as: $A = 0.736$, $\alpha = 0.147$,

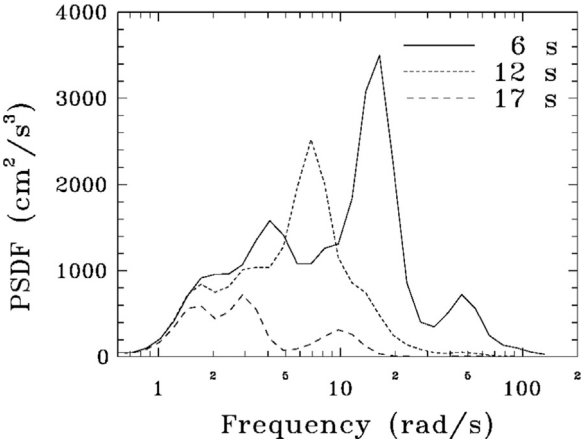

Fig. 5. Instantaneous PSDFs at different instants for the example motion.

$k = 5210$ m, $f_0 = 1.09$ Hz, and $b = 2.78$, as suggested by Harichandran and Vanmarcke [2] for Event # 20 at the SMART-1 array. As regards the apparent velocity v_{app}, values ranging from 2400 to 4500 m/s have been estimated during different events recorded at this array. However, for the present study, v_{app} is assumed to be 2500 m/s in order to emphasize the effects of spatial variability on the simulated motions.

At each of the four stations, an ensemble of 20 records is simulated. Fig. 6 shows the synthesized accelerograms corresponding to $r_{ij} = 0$, 100, 200, and 300 m for Stations 1–4. It may be seen that the simulated time histories look very similar to the original motion (see Fig. 2) in terms of temporal development.

The 5% damping (ensemble-averaged) response spectra for the simulated motions at each station are compared with the target spectrum in Fig. 7(a). The coefficient of variation (COV) spectra for the pseudo spectral acceleration ordinates of these motions are

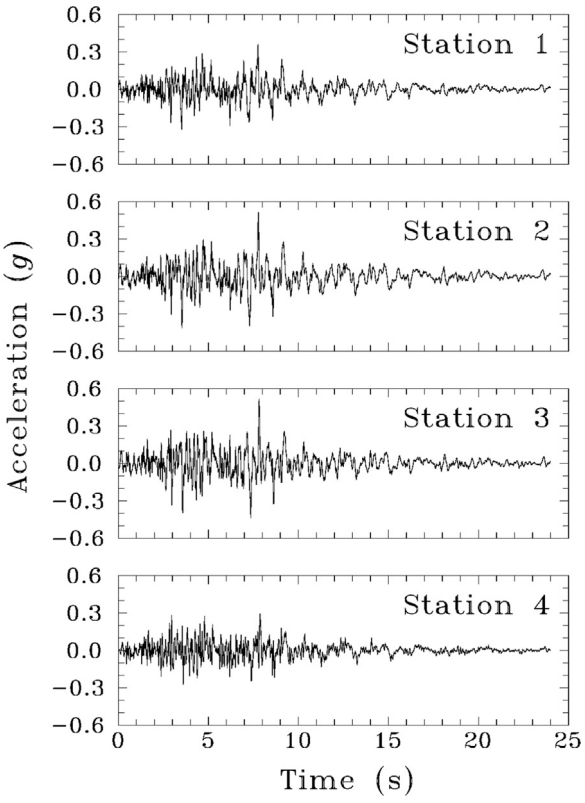

Fig. 6. Simulated ground motions at different stations with example motion characteristics.

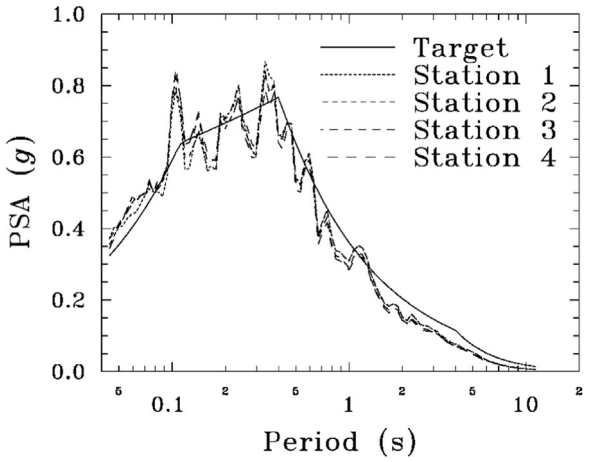

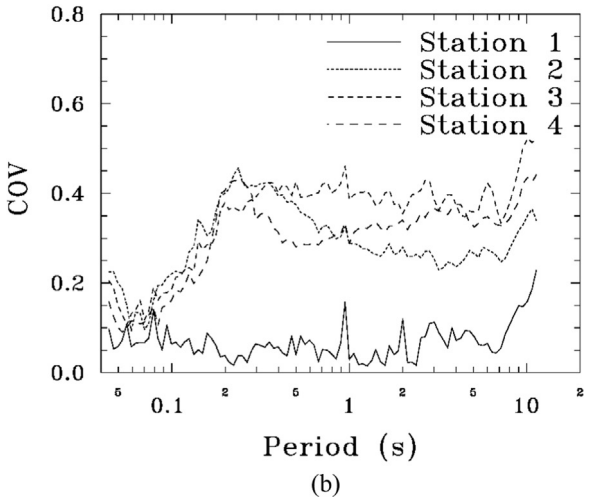

Fig. 7. Comparison of (a) mean response spectra for ensembles of simulated accelerograms at different stations with the target spectrum and (b) COV spectra for ensembles of simulated accelerograms at different stations.

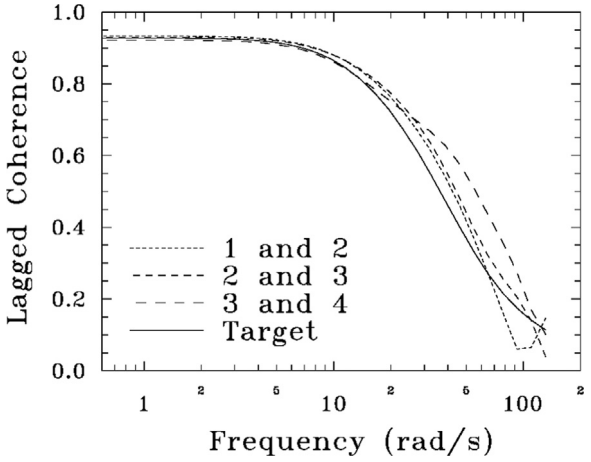

Fig. 8. Comparison of instantaneous lagged coherences for the ensemble of accelerograms at stations separated by 100 m with the target lagged coherence.

shown in Fig. 7(b). All the four response spectra appear to be in reasonably good agreement with the target spectrum, particularly for the periods between 0.1 and 1 s There is a little overestimation at shorter periods and underestimation at longer periods, possibly due to a large separation of 100–400 m between the four stations. Further, the three spectra for Stations 2–4 seem to be associated

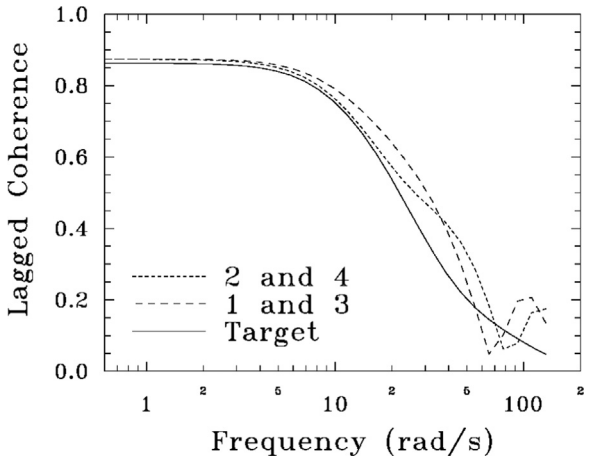

Fig. 9. Comparison of instantaneous lagged coherences for the ensemble of accelerograms at stations separated by 200 m with the target lagged coherence.

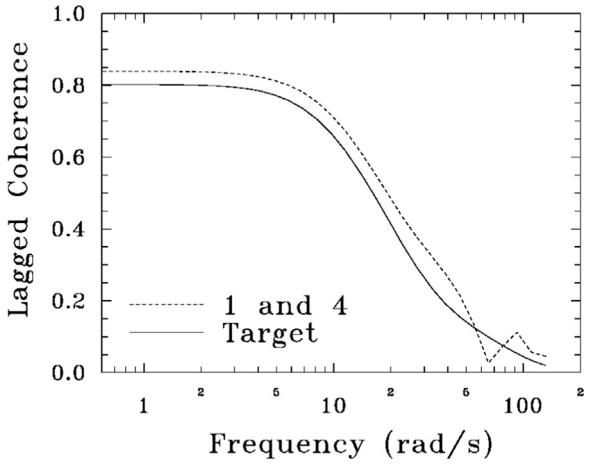

Fig. 10. Comparison of instantaneous lagged coherences for the ensemble of accelerograms at stations separated by 300 m with the target lagged coherence.

with significantly larger scatter, possibly as a manifestation of the interference of different wave components. The scatter is so prominent in Fig. 7(b) due to a low value of v_{app}, chosen intentionally to emphasize the effect of interference and wave propagation.

The instantaneous coherencies are also computed for each of the (six) pairs of stations by considering the ensembles of 20 accelerograms each. Figs. 8–10 show the comparisons for the absolute value of the instantaneous coherency function (which is same at all time instants) with the target lagged coherence (see Eqs. (36) and (37)). Fig. 8 is for the stations 100 m apart (Stations 1 and 2, Stations 2 and 3, Stations 3 and 4); Fig. 9 is for the stations 200 m apart (Stations 1 and 3, Stations 2 and 4); and Fig. 10 is for the stations 300 m apart (Stations 1 and 4). It may be observed that the computed instantaneous coherences are broadly in agreement with the target coherences.

5. Conclusions

A new method has been proposed to generate the ensembles of spatially correlated accelerograms at a given number of stations. The generated accelerograms at any station are consistent with a given response spectrum in the mean sense and incorporate nonstationary characteristics of a given accelerogram. The ensembles at any two stations are also made to satisfy a given coherency structure. It is assumed in the proposed formulation that

the same set of response spectra characterize the seismic hazard at all the stations.

The proposed method is based on the method of stochastic decomposition and spectral factorization technique, and the simulation is carried out through the estimation of wavelet coefficients. For this, a complex analytic mother wavelet has been obtained by generalizing the modified L-P wavelet function. This wavelet function is used to decouple the amplitude and phase information of a signal, and this is able to decompose a signal into component time-histories having energy in non-overlapping frequency bands. An expression for the instantaneous cross-PSDF has also been derived for the wavelet-based formulation.

The proposed formulation has been illustrated by generating the ensembles of accelerograms at four stations 100 m apart corresponding to the USNRC design spectrum and the nonstationary characteristics of a 1994 Northridge earthquake motion. It has been assumed for the numerical study that there are no temporal variations in the coherency structure between any two stations. It is observed that the simulated motions preserve the nonstationary characteristics of the example processes and the specified coherency structure at different instants of time. Also, the ensemble of generated motions at each of the stations is broadly compatible with the target design spectrum in the mean sense.

The proposed formulation takes care of the frequency nonstationarity without putting any limitation on the target process to be used for this purpose, and any recorded accelerogram may be used irrespective of the nature of the target response spectrum. The simulated motions can be easily made compatible with different design spectra at different stations in the case of large sites. Additionally, the proposed formulation has the flexibility of including temporal variations in the correlation structure as and when those become available and are considered to be important for application.

Appendix A. Methodology of Mukherjee and Gupta [46]

The main idea of the method of Mukherjee and Gupta [46] is to decompose a given earthquake accelerogram into sufficient number of time-histories having energy in non-overlapping frequency bands and then to scale those component time-histories iteratively for matching with a given response spectrum. The recorded accelerogram $f(t)$ is thus decomposed into N number of time-histories, i.e.,

$$f(t) = \sum_{j=1}^{N} f_j(t) \tag{31}$$

where $f_j(t)$ is the jth time-history given as

$$f_j(t) = \frac{K\Delta b}{a_j} \sum_i W_\psi f(a_j, b_i) \psi\left(\frac{t - b_i}{a_j}\right) \tag{32}$$

and N is such that $f_1(t)$, $f_2(t)$, …, $f_N(t)$ cover the entire frequency range of significant energy in $f(t)$. Further, various constants in Eq. (32) are same as explained in Section 2, and $\psi(t)$ is the modified L-P wavelet as in Eq. (6).

The time-history $f_j(t)$ is iteratively scaled as

$$f_j^{(n+1)}(t) = f_j^{(n)}(t) \frac{\int_{2a_j/\sigma}^{2a_j} \left[\mathrm{PSA}(T)\right]_{\text{target}} \mathrm{d}T}{\int_{2a_j/\sigma}^{2a_j} \left[\mathrm{PSA}^{(n)}(T)\right]_{\text{calculated}} \mathrm{d}T} \tag{33}$$

where $[\mathrm{PSA}(T)]_{\text{target}}$ is the ordinate of the target response spectrum at the period T, and $[\mathrm{PSA}^{(n)}(T)]_{\text{calculated}}$ is the ordinate of the response spectrum calculated from $f^{(n)}$ $(= \sum_{j=1}^{N} f_j^{(n)})$ at the same T after n iterations. The iterative process is continued for all N component time-histories till the error in the calculated response spectrum, as averaged over the chosen control time-periods, falls below a specified tolerance level.

Appendix B. Coherency function

Spatial variability is usually characterized by a (frequency-dependent) coherency function, which is in turn defined in terms of the cross-spectral density function and power spectral density functions of the processes involved. If $S_{xy}(\omega)$ denotes the cross-spectral density function of $\mathbf{x}(t)$ and $\mathbf{y}(t)$, and $S_x(\omega)$ and $S_y(\omega)$ denote the power spectral density functions of these processes respectively, the coherency function is defined as

$$\gamma_{xy}(\omega) = \frac{S_{xy}(\omega)}{\sqrt{S_x(\omega) S_y(\omega)}} \tag{34}$$

$\left|\gamma_{xy}(\omega)\right|^2$ describes the extent of correlation between $\mathbf{x}(t)$ and $\mathbf{y}(t)$ with $0 \le \left|\gamma_{xy}(\omega)\right|^2 \le 1$. In the case of $\mathbf{x}(t)$ and $\mathbf{y}(t)$ representing the ground acceleration processes at two stations, the (complex) coherency function can be either derived based on the theoretical considerations or obtained empirically from the ground motion data recorded by a dense array of accelerograph stations. This function is usually modeled as

$$\gamma_{xy}(\omega) = \rho(r_{xy}, f) \exp\left[\frac{i\omega r_{xy}}{v_{\text{app}}}\right] \tag{35}$$

where v_{app} is the apparent velocity of propagation of seismic waves at the site under consideration, $f = \omega/2\pi$ is the wave frequency in Hz, and $\rho(r_{xy}, f)$ is the frequency-dependent coherence. The exponential term in the above equation describes the wave-passage effect, i.e., the delay in the arrival of the waveforms at a station r_{xy} distance away due to their propagation. The other part, $\rho(r_{xy}, f)$, is a measure of the "similarity" in the seismic motions at the two stations and indicates the degree to which the two processes are related by means of linear transformation. It is expected that at low frequencies and short separation distances, the two processes will be almost similar, and therefore, $\rho(r_{xy}, f)$ will tend to unity as $\omega \to 0$ and $r_{xy} \to 0$. On the other hand, at large frequencies or at large separation distances, the motions are expected to be uncorrelated, and hence $\rho(r_{xy}, f)$ will tend to be zero. The value of correlation in between the two extreme cases will decay with frequency and separation distance. This observation has been validated by several analyses of recorded data, and different functional forms have been proposed in the recent years to describe the spatial variability empirically.

One of the popular coherence models has been proposed by Harichandran and Vanmarcke [2]. This model is based on the analyses of the SMART-1 array strong motion data and has the following form:

$$\begin{aligned}\rho(r_{xy}, f) &= A \exp\left[-\frac{2r_{xy}}{\alpha\theta(f)}(1 - A + \alpha A)\right] \\ &\quad + (1 - A) \exp\left[-\frac{2r_{xy}}{\theta(f)}(1 - A + \alpha A)\right]\end{aligned} \tag{36}$$

where

$$\theta(f) = k\left[1 + \left(\frac{f}{f_0}\right)^b\right]^{-1/2} \tag{37}$$

represents the frequency-dependent spatial scale of fluctuations; and A, α, k, f_0, and b are the parameters estimated by the regression analyses of the recorded data.

References

[1] Loh CH. Analysis of the spatial variation of seismic waves and ground movements from SMART-1 data. Earthq Eng Struct Dyn 1985;13(5):561–81.
[2] Harichandran RS, Vanmarcke EH. Stochastic variation of earthquake ground motion in space and time. J Eng Mech 1986;112(2):154–74 ASCE.
[3] Luco JE, Wong HL. Response of a rigid foundation to a spatially random ground motion. Earthq Eng Struct Dyn 1986;14(6):891–908.
[4] Loh CH, Yeh YT. Spatial variation and stochastic modelling of seismic differential ground movement. Earthq Eng Struct Dyn 1988;16(4):583–96.
[5] Somerville PG, McLaren JP, Saikia CK, Helmberger DV. Site-specific estimation of spatial incoherence of strong ground motion. In: Proceedings of the earthquake engineering and soil dynamics II—recent advances in ground motion evaluation, New York (U.S.A): Geotechnical Special Publication No. 20, ASCE; 1988.
[6] Abrahamson NA, Schneider JF, Stepp JC. Empirical spatial coherency functions for application to soil-structure interaction analyses. Earthq Spectra 1991;7(1):1–27.
[7] Hao H, Oliveira CS, Penzien J. Multiple-station ground motion processing and simulation based on SMART-1 array data. Nucl Eng Des 1989;111(3):293–310.
[8] Loh C-H, Lin S-G. Directionality and simulation in spatial variation of seismic waves. Eng Struct 1990;12(2):134–43.
[9] Abrahamson N, Schneider JF, Stepp JC. Spatial coherency of shear waves from the Lotung, Taiwan large-scale seismic test. Struct Saf 1991;10(1–3):145–62.
[10] Oliveira CS, Hong H, Penzien J. Ground motion modeling for multiple-input structural analysis. Struct Saf 1991;10(1–3):79–93.
[11] Der Kiureghian A. A coherency model for spatially varying ground motions. Earthq Eng Struct Dyn 1996;25(1):99–111.
[12] Zerva A, Harada T. Effect of surface layer stochasticity on seismic ground motion coherence and strain estimates. Soil Dyn Earthq Eng 1997;16(7–8):445–57.
[13] Yang Q-S, Chen Y-J. A practical coherency model for spatially varying ground motions. Struct Eng Mech 2000;9(2):141–52.
[14] Deodatis G. Simulation of ergodic multivariate stochastic processes. J Eng Mech 1996;122(8):778–87 ASCE.
[15] Zerva A. Response of multi-span beams to spatially incoherent seismic ground motions. Earthq Eng Struct Dyn 1990;19(6):819–32.
[16] Zerva A. On the spatial variation of seismic ground motions and its effects on lifelines. Eng Struct 1994;16(7):534–46.
[17] Shrikhande M, Gupta VK. Synthesizing ensembles of spatially correlated accelerograms. J Eng Mech 1998;124(11):1185–92 ASCE.
[18] Zerva A, Katafygiotis LS. Selection of simulation scheme for the nonlinear seismic response of spatial structures. In: Proceedings of the fourth international colloquium on computation of shell and spatial structures, Chania (Greece): IASS-IACM 2000; 2000.
[19] Spanos PD, Zeldin BA. Efficient iterative ARMA approximation of multivariate random processes for structural dynamics applications. Earthq Eng Struct Dyn 1996;25(5):497–507.
[20] Ramadan O, Novak M. Simulation of spatially incoherent random ground motions. J Eng Mech 1993;119(5):997–1016 ASCE.
[21] Ramadan O, Novak M. Simulation of multidimensional, anisotropic ground motions. J Eng Mech 1994;120(8):1773–85 ASCE.
[22] Li Y, Kareem A. Simulation of multivariate nonstationary random processes by FFT. J Eng Mech 1991;117(5):1037–58 ASCE.
[23] Li Y, Kareem A. Simulation of multivariate nonstationary random processes: hybrid DFT and digital filtering approach. J Eng Mech 1997;123(12):1302–10 ASCE.
[24] Vanmarcke EH, Heredia-Zavoni E, Fenton GA. Conditional simulation of spatially correlated earthquake ground motion. J Eng Mech 1993;119(11):2333–52 ASCE.
[25] Jin S, Lutes LD, Sarkani S. Efficient simulation of multidimensional random fields. J Eng Mech 1997;123(10):1082–9 ASCE.
[26] Heredia-Zavoni E, Santa-Cruz S. Conditional simulation of a class of nonstationary space-time random fields. J Eng Mech 2000;126(4):398–404 ASCE.
[27] Liao S, Zerva A. Physically-compliant, conditionally simulated spatially variable seismic ground motions for performance-based design. Earthq Eng Struct Dyn 2006;35(7):891–919.
[28] Shinozuka M. Simulation of multivariate and multidimensional random processes. J Acoust Soc Am 1971;49(1B):357–67.
[29] Zerva A. Spatial variation of seismic ground motions: modeling and engineering applications. London: Taylor & Francis; 2009.
[30] Ohsaki Y. On the significance of phase content in earthquake ground motions. Earthq Eng Struct Dyn 1979;7(5):427–39.
[31] Nigam NC. Phase properties of a class of random processes. Earthq Eng Struct Dyn 1982;10(5):711–7.
[32] Bi K, Hao H. Modelling and simulation of spatially varying earthquake ground motions at sites with varying conditions. Probab Eng Mech 2012;29:92–104.
[33] Konakli K, Der Kiureghian A. Simulation of spatially varying ground motions including incoherence, wave-passage and differential site-response effects. Earthq Eng Struct Dyn 2012;41(3):495–513.
[34] Cacciola P, Deodatis G. A method for generating fully nonstationary and spectrum-compatible ground motion vector processes. Soil Dyn Earthq Eng 2011;31(3):351–60.
[35] Zhang D-Y, Liu W, Xie W-C, Pandey MD. Modeling of spatially correlated, site-reflected, and nonstationary ground motions compatible with response spectrum. Soil Dyn Earthq Eng 2013;55:21–32.
[36] Shields MD. Simulation of spatially correlated nonstationary response spectrum-compatible ground motion time histories. J Eng Mech 2015;141(6):04014161 ASCE.
[37] Wen YK, Gu P. Description and simulation of nonstationary processes based on Hilbert spectra. J Eng Mech 2004;130(8):942–51 ASCE.
[38] Daubechies I. Ten lectures on wavelets. Philadelphia: Society for Industrial & Applied Mathematics; 1992.
[39] Newland DE. An introduction to random vibrations, spectral and wavelet analysis. Harlow: Longman; 1993.
[40] Basu B, Gupta VK. Non-stationary seismic response of MDOF systems by wavelet transform. Earthq Eng Struct Dyn 1997;26(12):1243–58.
[41] Basu B, Gupta VK. Seismic response of SDOF systems by wavelet modelling of nonstationary processes. J Eng Mech 1998;124(10):1142–50 ASCE.
[42] Basu B, Gupta VK. Wavelet-based analysis of the non-stationary response of a slipping foundation. J Sound Vib 1999;222(4):547–63.
[43] Basu B, Gupta VK. Stochastic seismic response of single-degree-of-freedom systems through wavelets. Eng Struct 2000;22(12):1714–22.
[44] Chatterjee P, Basu B. Non-stationary seismic response of tanks with soil interaction by wavelets. Earthq Eng Struct Dyn 2001;30(10):1419–37.
[45] Chatterjee P, Basu B. Wavelet analytic non-stationary seismic response of tanks. ISET J Earthq Technol 2003;40(1):61–75.
[46] Mukherjee S, Gupta VK. Wavelet-based generation of spectrum-compatible time-histories. Soil Dyn Earthq Eng 2002;22(9):799–804.
[47] Mukherjee S, Gupta VK. Wavelet-based characterization of design ground motions. Earthq Eng Struct Dyn 2002;31(5):1173–90.
[48] Zeldin BA, Spanos PD. Random field representation and synthesis using wavelet bases. J Appl Mech 1996;63(4):946–52 ASCE.
[49] Spanos PD, Failla G. Evolutionary spectra estimation using wavelets. J Eng Mech 2004;130(8):952–60 ASCE.
[50] Huang G, Chen X. Wavelets-based estimation of multivariate evolutionary spectra and its application to nonstationary downburst winds. Eng Struct 2009;31(4):976–89.
[51] Iyama J, Kuwamura H. Application of wavelets to analysis and simulation of earthquake motions. Earthq Eng Struct Dyn 1999;28(3):255–72.
[52] Gurley K, Kareem A. Applications of wavelet transforms in earthquake, wind and ocean engineering. Eng Struct 1999;21(2):149–67.
[53] Cecini D, Palmeri A. Spectrum-compatible accelerograms with harmonic wavelets. Comput Struct 2015;147:26–35.
[54] Giaralis A, Spanos PD. Wavelet-based response spectrum compatible synthesis of accelerograms—Eurocode application (EC8). Soil Dyn Earthq Eng 2009;29(1):219–35.
[55] Huang G. An efficient simulation approach for multivariate nonstationary process: Hybrid of wavelet and spectral representation method. Probab Eng Mech 2014;37:74–83.
[56] Sarkar K. Wavelet-based generation of spatially correlated accelerograms [MTech Thesis]. Kanpur, India: Department of Civil Engineering, IIT Kanpur; 2005.
[57] Grossman A, Morlet J. Decomposition of Hardy functions into square integrable wavelets of constant shape. SIAM J Math Anal 1984;15(4):723–36.
[58] Mallat S. A wavelet tour of signal processing. New York: Academic Press; 1998.
[59] Tatsuoka MM. Multivariate analysis. New York: John Wiley and Sons; 1971.
[60] Shinozuka M. Stochastic fields and their digital simulation. In: G. I. Schuëller, M. Shinozuka (Eds), Stochastic methods in structural dynamics, Dordrecht (The Netherlands): Springer; 1987.
[61] Cacciola P, Zentner I. Generation of response-spectrum-compatible artificial earthquake accelerograms with random joint time-frequency distributions. Probab Eng Mech 2012;28:52–8.
[62] Cacciola P. A stochastic approach for generating spectrum compatible fully nonstationary earthquakes. Comput Struct 2010;88(15–16):889–901.
[63] Deodatis G. Non-stationary stochastic vector processes: Seismic ground motion applications. Probab Eng Mech 1996;11(3):149–67.